

Development and Validation of a Simple Frozen Soil Parameterization Scheme Used for Climate Model

Zhang Yu (张宇)^① and Lu Shihua (吕世华)

Cold and Arid Regions Environment and Engineering Research Institute, Chinese Academy of Sciences, Lanzhou 730000

(Received June 7, 2001; revised November 26, 2001)

ABSTRACT

A simple frozen soil parameterization scheme is developed based on NCAR LSM and the effects of revised scheme are investigated using Former Soviet Union (FSU) 6 stations measurement data. In the revised model, soil ice content and the energy change in phase change process is considered; the original soil thermal conductivity scheme is replaced by Johanson scheme and the soil thermal and hydraulic properties is modified depending on soil ice content. The comparison of original model with revised model results indicates that the frozen soil scheme can reasonably simulate the energy budget in soil column and the variation of thermal and hydraulic properties as the soil ice content changes. Soil moisture in spring is decreased because of the reduction of infiltration and increment of runoff. Consequently, the partition of heat flux and surface temperature changes correspondingly.

Key words: Frozen soil parameterization, Land surface model, Climate model

1. Introduction

The impact of the winter season processes on regional and global general circulation has been paid more and more attention recently. Frozen soil process plays an important role in the hydrology of cold regions. Ice forms in the spaces between soil particles. As the ice content increases, the open channels between soil particles become narrow, and directly restrict infiltration of surface water. Aside from this, soil ice also changes the soil thermal properties. The thermal conductivity of water is $0.57 \text{ W m}^{-1} \text{ K}^{-1}$, while that of ice is $2.2 \text{ W m}^{-1} \text{ K}^{-1}$. A frozen soil with ice content has a higher thermal conductivity than a soil with equivalent content of liquid water. The volumetric heat capacity for water is $4.2 \times 10^6 \text{ J m}^{-3} \text{ K}^{-1}$, while it is $1.9 \times 10^6 \text{ J m}^{-3} \text{ K}^{-1}$ for ice. So increasing of the soil ice content decreases its thermal storage capacity and influences the transfer of soil flux. Simultaneously, absorbing and releasing latent heat can redistribute the soil heat when water phase changes.

In the earlier numerical simulation on frozen soil process, Harlan (1973), Guymon and Luthin (1974) and Jame and Norum (1980) simulated the freezing/thawing process through evaluation of water and heat transfer equations. These models require high-resolution finite difference schemes and computationally expensive iterative techniques and time steps with only a few seconds, so they were hardly employed in climate models. Kennedy and Sharatt (1998) compared four schemes for simulating frozen front, and found that the finite difference schemes were better than others and heat transfer in soil column was very sensitive to snow depth simulation.

^①E-mail: yuzhang@ns.lzb.ac.cn

In more sophisticated Land Surface Scheme (LSS), there is some consideration about effects on thermal and hydraulic properties of soil ice. In BATS (Dickinson et al. 1993), it assumes that water in the soil freezes uniformly between 0 and -4°C , and the thermal diffusivity of the soil is limited to $1.4 \times 10^{-6} \text{ m}^2 \text{ s}^{-1}$. Additionally the frozen soil moisture is assigned a lower volumetric heat capacity and heat is added to the upper soil layer to consider the latent heat of fusion. In SSiB (Xue et al. 1996), if the temperature of the third soil layer is below freezing, all liquid precipitation is diverted into runoff. Sellers et al. (1996) modified the hydraulic conductivity $K_{\text{frz}} = K_{\text{H}} [T_{\text{soil}} - (T_{\text{frz}} - 10)] / 10$. In BASE (Slater et al. 1998), it also considers the effects of frozen soil.

There are more complex frozen soil parameterization schemes recently. Cherkauer and Lettenmaier (1999) considered absorbing/releasing process when soil water was thawing/freezing, and employed Johanson (1975) thermal conductivity method, and validated with the Mississippi River Basin data. Pauwels and Wood (1999) developed simple snow and frozen soil scheme and validated it using BOREAS data. Koren et al. (1999) developed a new frozen soil parameterization based on NCEP/OSU LSM, and found that neglecting frozen soil process can result in simulated high/cold bias in freezing/thawing period. There are 11 land schemes that consider effects of frozen soil in total 21 land models that take part in PILPS 2(d). It is found that small temperature differences in frozen soil can subsequently lead to large ground and surface heat flux differences (Schlosser et al. 2000).

In the study, we try to develop a relative complex frozen soil scheme and investigate the effects of frozen soil in the land surface model based on NCAR LSM. There are two reasons that we select this model: (1) there is more sophisticated consideration on other components; and (2) it is convenient to be coupled to the Community Climate Model.

2. Development of frozen soil parameterization scheme

2.1 Original NCAR Land Surface Model (LSM)

The model is a one-dimensional model of energy, momentum, water, and CO_2 exchange between atmosphere and the land, accounting for ecological differences among vegetation types, hydraulic and thermal differences among soil types, and allowing for multiple surface types, including lakes and wetlands within a grid cell. Some features of the model are prescribed time-varying leaf and stem areas; absorption, reflection, and transmittance of solar radiation, accounting for the different optical properties of vegetation, soil, water, snow, and ice; sensible heat and latent heat, partitioning latent heat into canopy evaporation, soil evaporation, and transpiration from sunlit and shaded foliage; temperature for a six-layer soil column using a heat diffusion equation that accounts for phase change; soil water for the same six-layer soil column using a one-dimensional conservation equation that accounts for infiltration input, gravitational drainage at the bottom of the column. The details about the model can refer to Bonan (1996). Resolution of the heat and water transfer equations and the parameterization of thermal and hydraulic properties are described below.

2.1.1 Resolution of heat and water transfer equations

The one-dimensional for energy conservation equation is

$$c \frac{\partial T}{\partial t} = - \frac{\partial F_z}{\partial z} = \frac{\partial}{\partial z} \left(k \frac{\partial T}{\partial z} \right), \quad (1)$$

where c is the volumetric soil heat capacity ($\text{J m}^{-3} \text{K}^{-1}$), T is the soil temperature (K), k is the thermal conductivity ($\text{W m}^{-1} \text{K}^{-1}$), and F_z is the heat flux (W m^{-2}) at depth z . The soil column is divided into six layers with thickness Δz_i of 0.1 m, 0.2 m, 0.4 m, 0.8 m, 1.6 m, and 3.2 m respectively. Every properties are defined at the center of each layer, and the energy balance for the i th layer is

$$\frac{c_i \Delta z_i}{\Delta t} (T_i^{n+1} - T_i^n) = -F_{i-1} + F_i \quad (2)$$

This equation is solved using the Crank–Nicholson method with the boundary conditions of G , as the heat flux into the soil column and zero heat flux at the bottom of the soil column.

Soil water is calculated from the conservation equation

$$\frac{\partial \theta}{\partial t} = \frac{\partial}{\partial t} \left[k \left(\frac{\partial \theta}{\partial z} \frac{\partial \psi}{\partial \theta} + 1 \right) \right] \quad (3)$$

It is still solved by the Crank–Nicholson method with boundary conditions of infiltration, soil evaporation and transpiration as the flux of water into the soil and gravitational drainage as the flux of water at the bottom of the soil column.

2.1.2 Parameterization of soil properties

2.1.2.1 Thermal properties

Soil thermal capacity varies linearly with soil moisture in the form

$$\begin{cases} c_u = (1 - \theta_{\text{sat}})c_s + c_w \theta_i \\ c_f = (1 - \theta_{\text{sat}})c_s + c_i \theta_i \end{cases} \quad (4)$$

where c_u and c_f are the unfrozen and frozen soil heat capacities, c_w and c_i are the heat capacities of water and ice, respectively, c_s is the heat capacity of soil solids, θ_i is the volumetric water content of the i th soil layer, and θ_{sat} is the volumetric water content at saturation. Thermal volumetric capacity of i th soil layer is

$$c_i = \begin{cases} c_u & T_i > T_f + \Delta T \\ \frac{c_f + c_u}{2} + \frac{L_i}{2\Delta T} & T_f - \Delta T \leq T_i \leq T_f + \Delta T \\ c_f & T_i < T_f - \Delta T \end{cases} \quad (5)$$

where $\Delta T = 0.5 \text{ K}$, T_f is the freezing point, $L_i = \theta_i h_{\text{fus}} \rho_w$, θ_i is the volumetric soil water content ($\text{mm}^3 \text{mm}^{-3}$) of the i th soil layer, h_{fus} is the latent heat of fusion of water (J kg^{-1}), and ρ_w is the density of water (kg m^{-3}).

Thermal conductivity is a blend of frozen and unfrozen values over the temperature range $T_f \pm 0.5 \text{ K}$,

$$K_i = \begin{cases} k_u & T_i > T_f + \Delta T \\ k_f + \frac{k_u - k_f}{2\Delta T} (T_i - T_f + \Delta T) & T_f - \Delta T \leq T_i \leq T_f + \Delta T \\ k_f & T_i < T_f - \Delta T \end{cases} \quad (6)$$

The unfrozen k_u and frozen k_f thermal conductivity ($\text{W m}^{-1} \text{K}^{-1}$) are calculated from Farouki (1981)

$$\begin{cases} k_u = (k_s^{(1-\theta_{\text{sat}})}) k_w^{\theta_i} - 0.15 \frac{\theta_i}{\theta_{\text{sat}}} + 0.15 \\ k_f = (k_s^{(1-\theta_{\text{sat}})}) k_i^{\theta_i} - 0.15 \frac{\theta_i}{\theta_{\text{sat}}} + 0.15 \end{cases}, \quad (7)$$

where k_s , k_i and k_w are the thermal conductivities of soil solids, ice and water, respectively.

2.1.2.2 Hydraulic properties

The hydraulic conductivity κ_i and the soil matrix potential ψ_i vary with θ_i and soil texture based on the works of Clapp and Hornberger (1978) and Cosby et al. (1984). For the i th layer

$$\begin{cases} \kappa_i = \kappa_{\text{sat}} s_i^{2b+3} \\ \psi_i = \psi_{\text{sat}} s_i^{-b} \end{cases}, \quad (8)$$

where $s_i = \theta_i / \theta_{\text{sat}}$, the hydraulic conductivity at saturation κ_{sat} (mm s^{-1}), the matrix potential at saturation ψ_{sat} (mm), the water content at saturation θ_{sat} , and b are given by the empirical relation in Cosby et al. (1984).

2.2 Development of frozen soil parameterization

2.2.1 Thermal conductivity and volumetric heat capacity of frozen soil

We consider the following aspects of frozen soil effects: (1) latent heat releasing / absorbing in soil water freezing / thawing; (2) the influence on soil liquid water flow for existence of ice; (3) influence on infiltration of freezing ground surface; (4) the evaporation of the freezing ground surface.

Considering soil water phase change, the heat flux equation with a source / sink term is

$$c(\theta, \theta_{\text{ice}}) \frac{\partial T}{\partial t} = \frac{\partial}{\partial z} \left[k(\theta, \theta_{\text{ice}}) \frac{\partial T}{\partial z} \right] + \rho_w h_{\text{fus}} \frac{\partial \theta_{\text{ice}}}{\partial t}, \quad (9)$$

where θ is total volumetric soil moisture, θ_{ice} is soil ice content (ice water), and the other variables are the same as described above. Soil volumetric capacity is weighted by every component

$$c(\theta, \theta_{\text{ice}}) = (\theta - \theta_{\text{ice}}) c_w + \theta_{\text{ice}} c_i + (1 - \theta_{\text{sat}}) c_s, \quad (10)$$

where c_s , c_w , and c_i are volumetric heat capacity of soil solid, water and ice, respectively.

There are various methods to estimate frozen soil thermal conductivity. We adopted Johanson's (1975) method. As concluded by Peter-Lidard et al. (1998) and Farouki (1986), it is the most accurate over the full range of saturation.

The method calculates the thermal conductivity of a soil as a function of its saturation, porosity, quartz content, and dry density and phase of water (frozen or unfrozen). The thermal conductivity is calculated as a combination of the dry conductivity k_{dry} and saturated k_{sat} thermal conductivity, weighted by a normalized thermal conductivity

$$k = K_e (k_{\text{sat}} - k_{\text{dry}}) + k_{\text{dry}}, \quad (11)$$

K_e is known as Kersten number. For natural soil

$$k_{\text{dry}} = \frac{0.135\gamma_d + 64.7}{2700 - 0.947\gamma_d} \quad (12)$$

where k_{dry} is in $\text{W m}^{-1} \text{K}^{-1}$, γ_d is the dry soil density in kg m^{-3} . In practice, the density may be obtained from the porosity θ_{sat} assuming the same solids unit weight as

$$\gamma_d = (1 - \theta_{\text{sat}})2700 \quad (13)$$

The saturated thermal conductivity k_{sat} depends on the porosity θ_{sat} , the quartz content q , and the unfrozen volume fraction x_u (which is defined as $\theta_{\text{sat}} \times (\theta - \theta_{\text{ice}}) / \theta$), i.e.,

$$k_{\text{sat}} = k_s^{1 - \theta_{\text{sat}}} k_i^{\theta_{\text{sat}} - x_u} k_w^{x_u} \quad (14)$$

where the thermal conductivity of ice $k_i = 2.2 \text{ W m}^{-1} \text{K}^{-1}$, the thermal conductivity of water $k_w = 0.57 \text{ W m}^{-1} \text{K}^{-1}$, the soil solids thermal conductivity k_s is given as

$$k_s = k_q^q k_o^{1-q} \quad (15)$$

where the thermal conductivity of quartz $k_q = 7.7 \text{ W m}^{-1} \text{K}^{-1}$, and the thermal conductivity of other mineral is given as $k_o = 2.0 \text{ W m}^{-1} \text{K}^{-1}$. We assume that all the sand is composed of quartz.

Kersten number is a function only of the degree of saturation S_r and phase of the water. For unfrozen soils,

$$K_e = \begin{cases} 0.7 \log S_r + 1.0 & S_r > 0.05 \quad \text{coarse} \\ \log S_r + 1.0 & S_r > 0.1 \quad \text{fine} \end{cases} \quad (16)$$

In this paper, all soil type was assumed as fine soil. For frozen soils,

$$K_e = S_r \quad (17)$$

Figure 1 is comparison of original scheme for thermal conductivity (Farouki 1981) and revised scheme under loam soil type.

2.2.2 Resolution of ice content

Following Koren et al. (1999)'s scheme, the ice content at each soil layer is estimated as a function of soil temperature and total soil moisture content. It is assumed that when ice is present, soil water potential remains in equilibrium with the vapor pressure over pure ice. A simple relation, based on the Clausius-Claperyron equation for phase equilibrium, can be drawn between the freezing point of soil water and the soil water potential ψ , after neglecting soil water osmotic potential $\psi = \frac{h_{\text{fus}}(T - T_f)}{gT}$, where g is the acceleration of gravity h_{fus} is the latent heat of fusion of water (J kg^{-1}). Campell's relationship between water potential and water content was modified to account for the effects of frozen soil.

$$\psi(\theta, \theta_{\text{ice}}) = \psi_s \left(\frac{\theta - \theta_{\text{ice}}}{\theta_s} \right)^{-b} (1 + c_k \theta_{\text{ice}})^2 \quad (18)$$

where parameter c_k accounts for the effect of increase in specific surface of soil minerals and ice-liquid water; the average value of this parameter is 8. Combining above two equation leads to

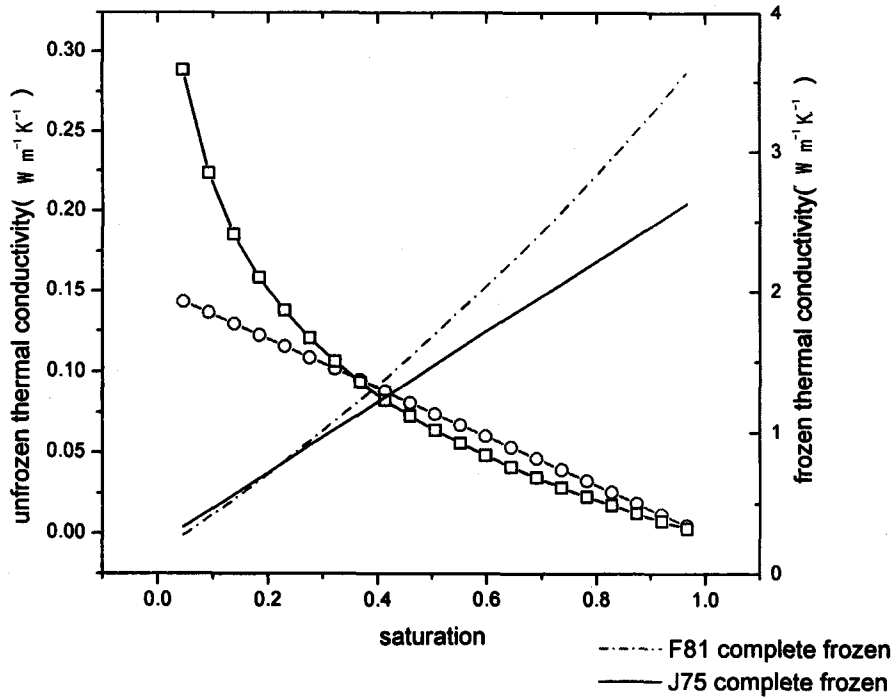


Fig. 1. Comparison of thermal conductivity parameterization of Farouki (1981) and Johanson (1975) under loam soil type.

$$\frac{g\psi_s}{L} (1 + c_k \theta_{ice})^2 \left(\frac{\theta - \theta_{ice}}{\theta_s} \right)^{-b} - \frac{T - T_f}{T} = 0 . \tag{19}$$

From the equation, the ice content depends on soil temperature, soil moisture, and soil texture. We use iterative method to solve the equation.

2.2.3 Hydraulic conductivity of frozen soil

There are basic theories for the movement of moisture through the frozen soil. The first is that moisture can move through the soil via the unfrozen films presented on the soil particle surfaces. This is analogous to the moisture movement in unfrozen soils where the hydraulic conductivity and matrix potentials are the driving forces and Darcy's law is applied for moisture flow in equilibrium conditions. The second theory of the flow proposes that phase change is the main driving mechanism behind fluid flows. Here, we still adopted the first method on frozen soil flow, considering effects of ice on hydraulic conductivity and soil water potential in Eq.(3). Soil water potential was using relationship in Eq.(18). Based on the modification by O'Neill and Miller (1985) on hydraulic conductivity, we have

$$\kappa_{fs} = \kappa_s (\theta_h / \theta_{sat})^9 , \tag{20}$$

where κ_{fs} is hydraulic conductivity in saturation frozen soil, κ_s is hydraulic conductivity in saturation unfrozen soil, θ_h is liquid soil water content. For unsaturated frozen soil, we used relationship in Eq.(8), but κ_{sat} is replaced by κ_{fs} . Meanwhile, modification on hydraulic conductivity also affected the form of infiltration and runoff.

Saturation vapor pressure $e_*(T)$ and $\frac{de_*(T)}{dT}$, that are needed in calculating surface evaporation, are calculated using polynomials

$$100\{a_0 + T[a_1 + T(a_2 + T(a_3 + T(a_4 + T(a_5 + Ta_6))))]\}, \quad (21)$$

where the coefficients a_0 and a_6 vary for saturation vapor pressure with reference to water or ice (Bonan 1996).

3. Forcing data and experiment design

The data used in this study was described and used by Robock et al. (1995), from six hydrometeorological stations between 1978 and 1983 in Former Soviet Union (FSU). After that, the datasets were used in worldwide for their high quality and widespread geographical distribution (Uralsk, 51.3°N, 51.4°E; Ogurtsovo, 54.9°N, 82.9°E; Yershov, 51.4°N, 48.3°E; Kostroma, 57.8°N, 40.9°E; Khabarovsk, 48.5°N, 135.2°E; Tulun, 54.6°N, 100.6°E). Yang et al. (1997), Sun et al. (1999) used the data to validate the new snowpack parameterization, Slater (1998) used the data to investigate the effects of a new frozen soil scheme.

The meteorological part of these data included saturation deficiency, dew point temperature, cloudiness amount, wind direction, wind velocity, precipitation, air pressure, air temperature etc. The actinometric data included net radiation at the surface, direct short wave radiation, total incoming solar radiation etc. Both meteorological and actinometric data were observed every 3 hours. There was no observed downward longwave radiation, and we still adopt Satterlund bulk scheme, which was used in Robock et al. (1995), to calculate it,

$$L_D = \varepsilon_a [1 + 0.2(C_L + C_M)^2 + 0.4C_H^2] \sigma T_a^4, \quad (22)$$

where $\varepsilon_a = 1 - \exp(-e_a^{T_a/b})$, e_a is vapor pressure, $b = 2016$ K, total and low cloudiness amounts C_T and C_L are the measured data, middle and high cloudiness amount are $C_M = C_H = (C_T - C_L) / 2$.

We run the original LSM (OLSM) and revised version (RLSM) forced by six stations data to investigate the effects of frozen soil scheme in a land surface model. In each simulation, the models were initialized with 279 K in temperature and $0.35 \text{ m}^3 \text{ m}^{-3}$ in soil moisture, then

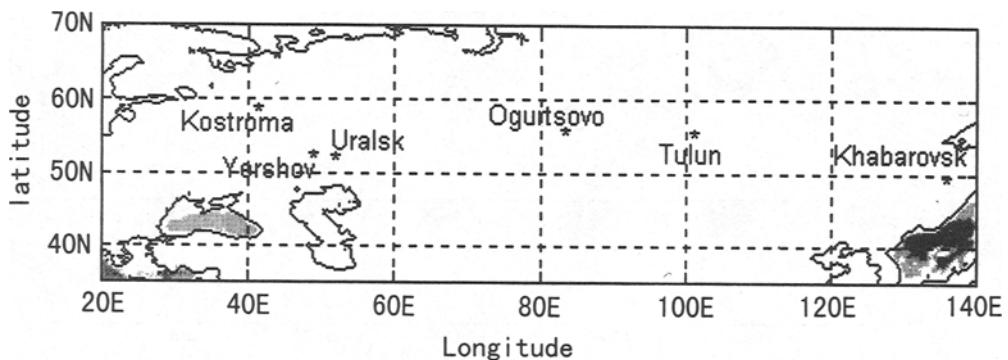


Fig. 2. Location of six stations used in this paper.

used the observed data of first year to spin-up the model until achieving equilibrium. In all cases, vegetation cover was chosen as grassland, for the soil type we adopted values used in CCM3 within the same grid. The vegetation and soil thermal and hydraulic parameters were parameterized using the scheme in the model.

Limited by the paper length, we only give the figures for Ogurtsov and Yershov station, the results of other stations are very similar to that of these two stations, except for some cool bias of Tulun station.

4. Simulations of original and revised model

4.1 Simulations of frozen depth

The frozen depth was mainly determined by soil temperature, and indirectly influenced by simulated soil moisture. For the low-resolution in the soil column and little ice existing above 0°C , we defined the $0.03 \text{ m}^3 \text{ m}^{-3}$ isoline of ice-liquid water content, which is very close to 0°C isotherm of soil temperature, as frozen depth. There are better simulation at Uralsk, Ogurtsovo, Yershov, Kostroma (Fig. 3), which can reflect the seasonal variation of frozen depth. All of these stations are located in the central continent and well simulated in the soil moisture, except for Ogurtsovo, which is in slightly wet region with worse simulation in soil moisture. For Khabarovsk and Tulun, the simulated freezing state is too strong and frozen depth is too deep (Figure omitted). One reason is that the air temperature is too low, below -20°C , and the observed frozen depth is very deep. The other reason is the bias in simulation of soil moisture.

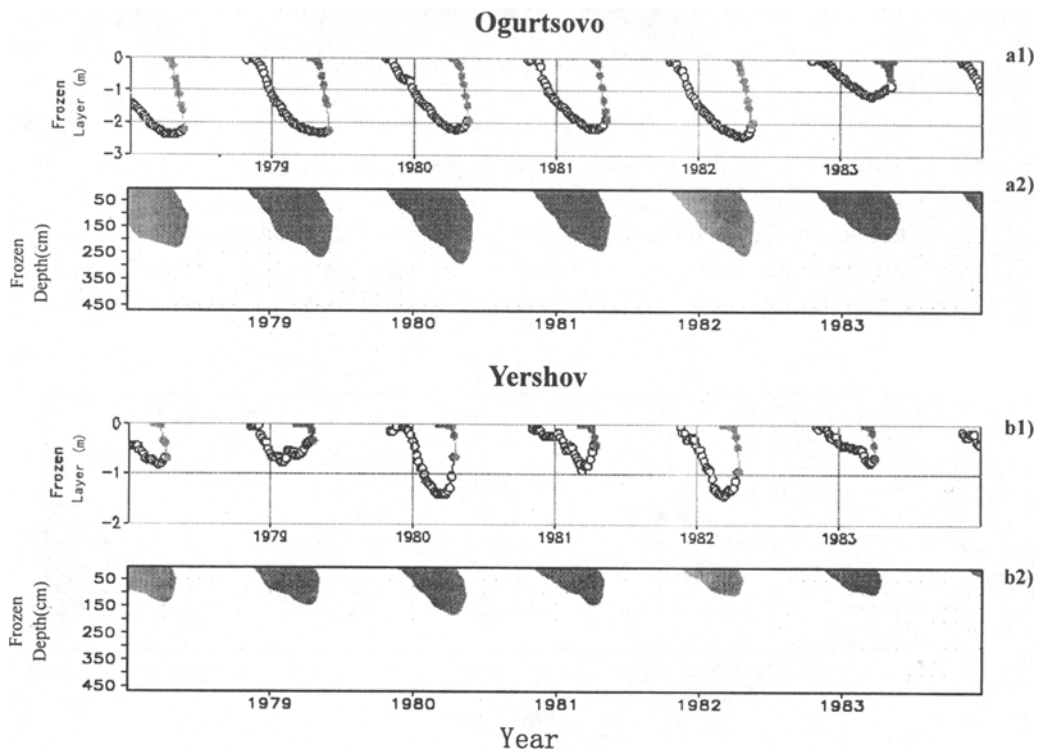


Fig. 3. Observed (a1 and b1) and simulated (a2 and b2 in which shaded part is greater than $0.03 \text{ m}^3 \text{ m}^{-3}$ for ice content) frozen depth of Ogurtsovo and Yershov.

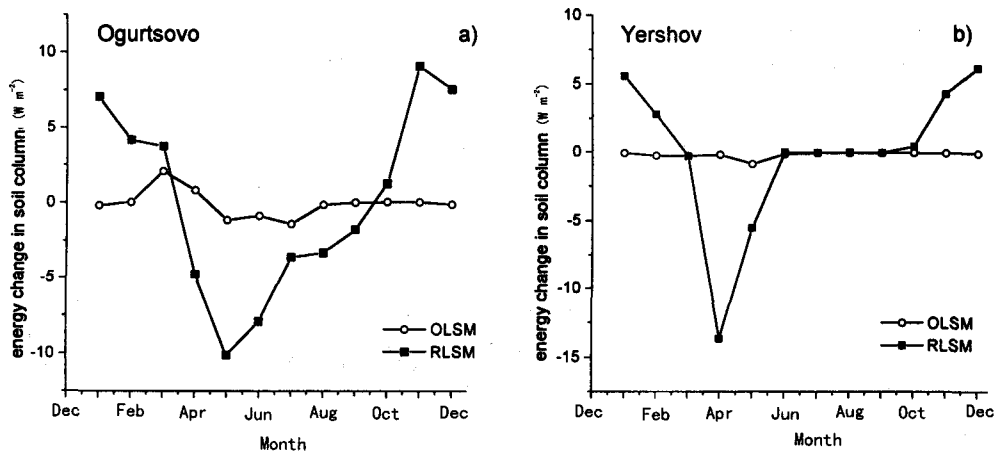


Fig. 4. 6-year monthly averaged energy change in soil column (W).

4.2 Simulation of soil thermal condition

The new scheme considers the phase change of soil water, that includes releasing / absorbing process in freezing / thawing period. Figure 4 is the energy increment in the soil column compared with previous time step, i.e. $\sum_i \frac{c_i \Delta z_i}{\Delta t} (T_i^{n+1} - T_i^n) - G$, where G is the ground heat flux. When there is no freezing or thawing occurrence, the energy is conserved in the soil column. For Yershov, the energy increment in the soil column is positive during the freezing period from November to February, and is negative during the thawing period, from March to May. However, for Ogurtsovo, the freezing period is from October to March, and the thawing period is from April to September. Thus, the revised model can simulate the energy change in the soil column reasonably.

From Eq.(5), the soil water phase change has been implicitly considered in the original model, i.e. when $T_f - \Delta T \leq T_i \leq T_f + \Delta T$, the latent heat of fusion of water is considered, and all of the soil moisture takes part in phase change, meanwhile, the existence of the liquid water in frozen soil is not taken into consideration. The method has overestimated the effects of the soil moisture phase change, and led to the cool bias in summer. Figure 5 shows the comparison between the simulated 20 cm soil temperature by OLSM and RLSM and the observed data. The simulation of RLSM is closer to the observed data than OLSM. Figure 6 is the comparison of simulated ground heat flux in each case, and it shows that the magnitude of RLSM is smaller than the OLSM's. For the ground heat flux, $G = \frac{2k_1}{\Delta z_1} (T_g - T_1)$, where k_1 is the thermal conductivity of the first soil layer, Δz_1 is the thickness of the first soil layer, and $T_g - T_1$ is the difference of temperature between ground and the first soil layer. Because the difference of $T_g - T_1$ between OLSM and RLSM is too small, the difference of ground flux may be caused by the modification of the thermal conductivity scheme.

4.3 Simulations of water cycle and surface heat flux

Figure 7 is the comparison of infiltration and runoff. After considering the frozen soil

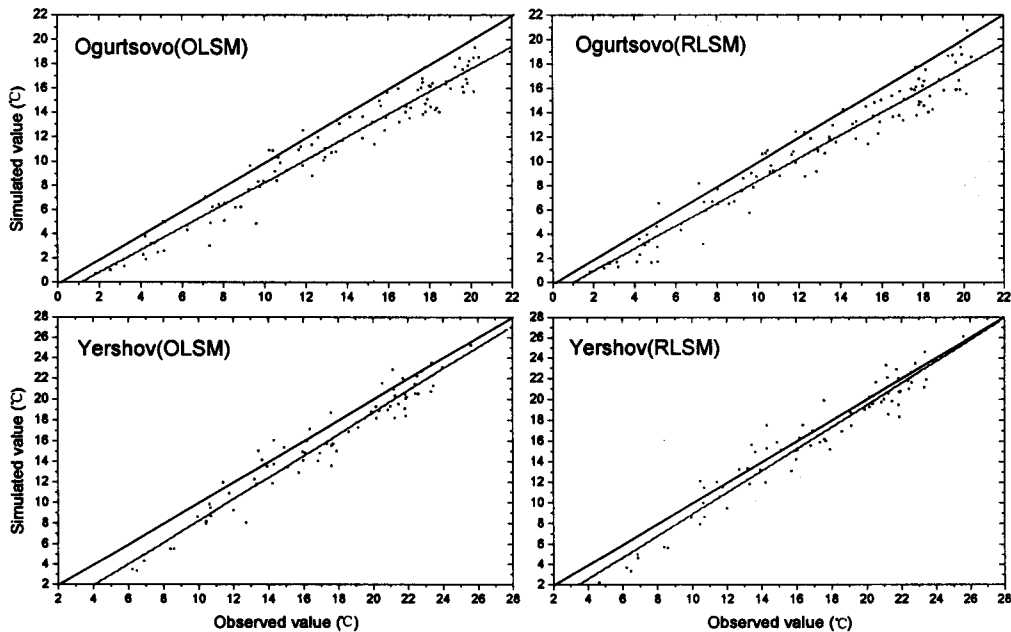


Fig. 5. Simulated (Y -axis) versus observed (X -axis) 20 cm soil temperature for two stations. The 1:1 line and linear regression line are plotted on each panel.

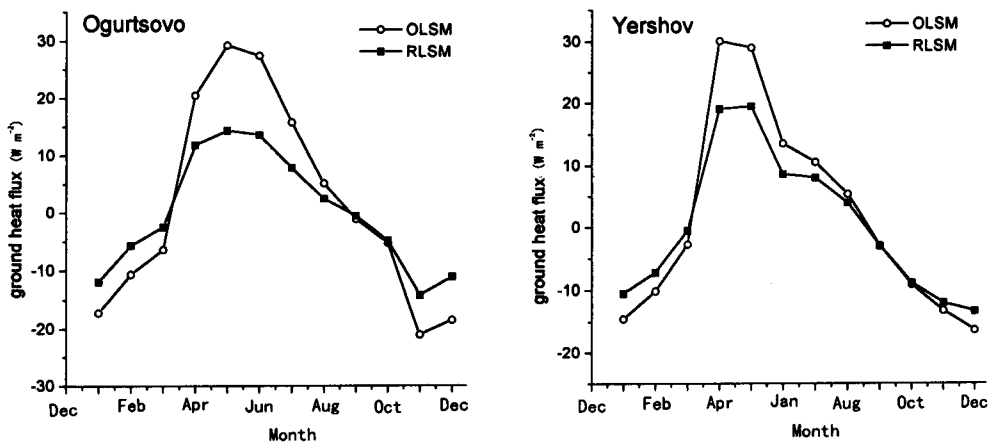


Fig. 6. 6-year monthly averaged ground heat flux ($W m^{-2}$).

process, the hydraulic conductivity of first soil layer is decreased, and the soil porosity turned small. Thus, during the spring snowmelt period, it is easy to form saturated surface runoff rather than forming infiltration. In later fall, there is a few runoff. In OLSM's simulation, the amount of infiltration is very large, and hardly to form runoff. There is no observed data about runoff; but the magnitude of RLSM modeled value is very closed to Valdai data (Schlosser et al. 2000). Figure 8 is 6-year averaged 0–50 cm available soil moisture

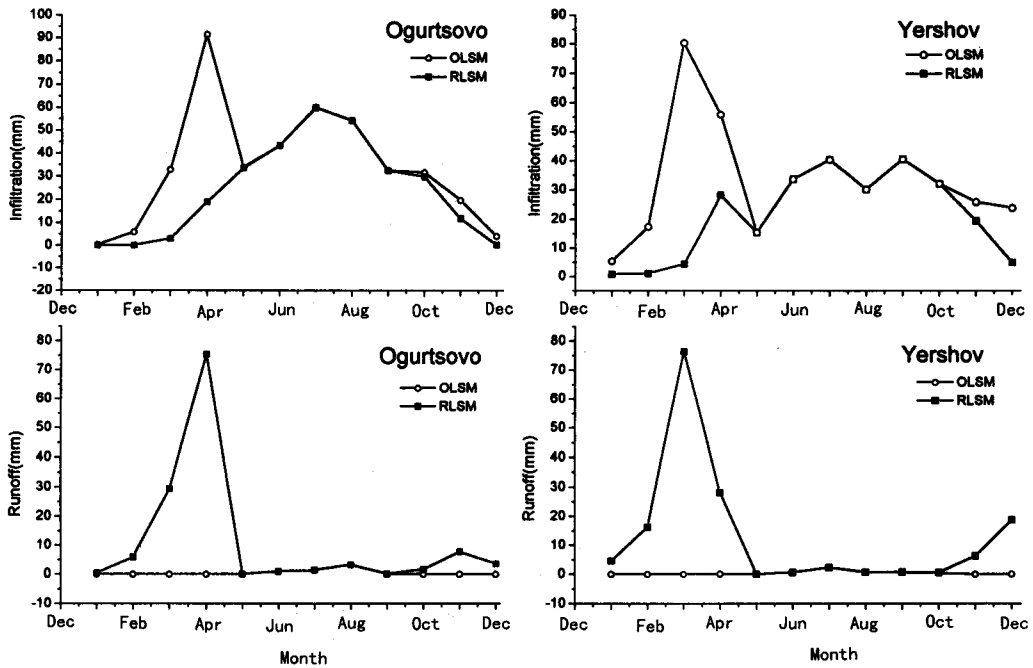


Fig. 7. 6-year monthly averaged infiltration and runoff for two stations (mm).

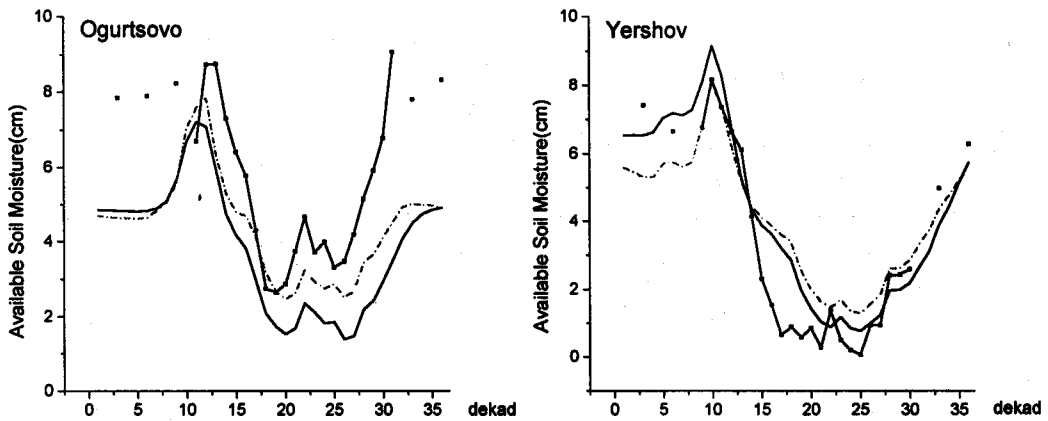


Fig. 8. 6-year averaged 0-50 cm available soil moisture (solid line with solid square is observed data; dash line for OLSM; solid line is for RLSM).

(ASM), $W_i = (\theta - \theta_{dry})D_i$, where W_i is the ASM, θ is the total soil moisture, θ_{dry} is the soil moisture when the soil is dry, and D_i is the depth of i th soil layer.

The results are very similar to Robock's (Robock et al. 1995, Fig. 7) simulation using Bucket and SSIB model. For Ogurtsovo, and Yershov, which are located in the center of continent, the results are similar and better than that for other stations. The OLSM can simulate

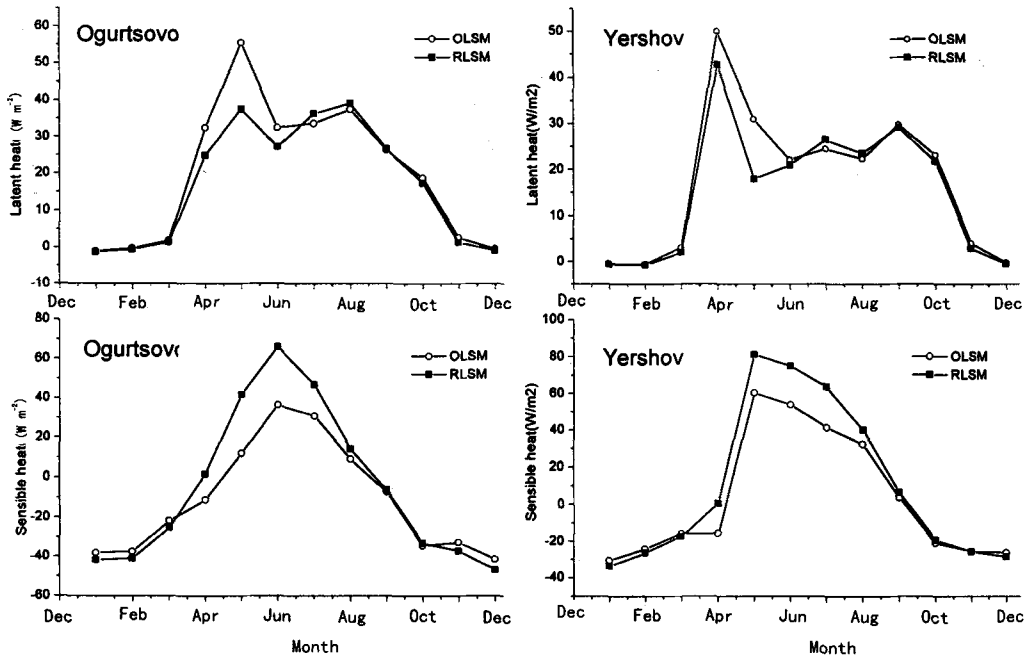


Fig. 9. 6-year monthly averaged latent heat and sensible heat $W m^{-2}$ (lines with open circle are for OLSM; lines with solid square are for RLSM).

the spike of ASM in spring; but in RLSM, when snowmelt occurs, the snowmelt forms runoff rather than infiltration because the ground is still frozen.

Because of the difference of simulated soil moisture between OLSM and RLSM, the simulated evaporation by RLSM is less than that by OLSM, and so do the latent heat (Fig. 9). Figure 10 is the comparison between simulated and observed ground temperature for OLSM and RLSM, from which we can see that, the simulated ground temperature by RLSM is slightly higher than that by OLSM in summer. Because of the larger temperature difference between the ground and the atmosphere, the simulated sensible heat by RLSM is higher than that by OLSM in spring and summer.

5. Conclusion and discussion

In this study, we develop a simple frozen soil parameterization scheme based on NCAR LSM. The soil ice content is solved; the sink / source effects of soil water phase-changing are considered; the thermal conductivity is modified for well solving water-ice mixed soil; the hydraulic conductivity is calculated depending on the soil ice content. Then some simulation experiments are conducted with the original model and revised model using Former Soviet Union 6 stations measured data.

The results indicate that the energy in the soil column increases during the freezing period, and decreases during the thawing period because of the latent heat releasing / absorbing when the soil water freezing / thawing. The simulated summer soil temperature by the revised model is closer to the observed data. When the snowmelt occurs in spring, the ground surface

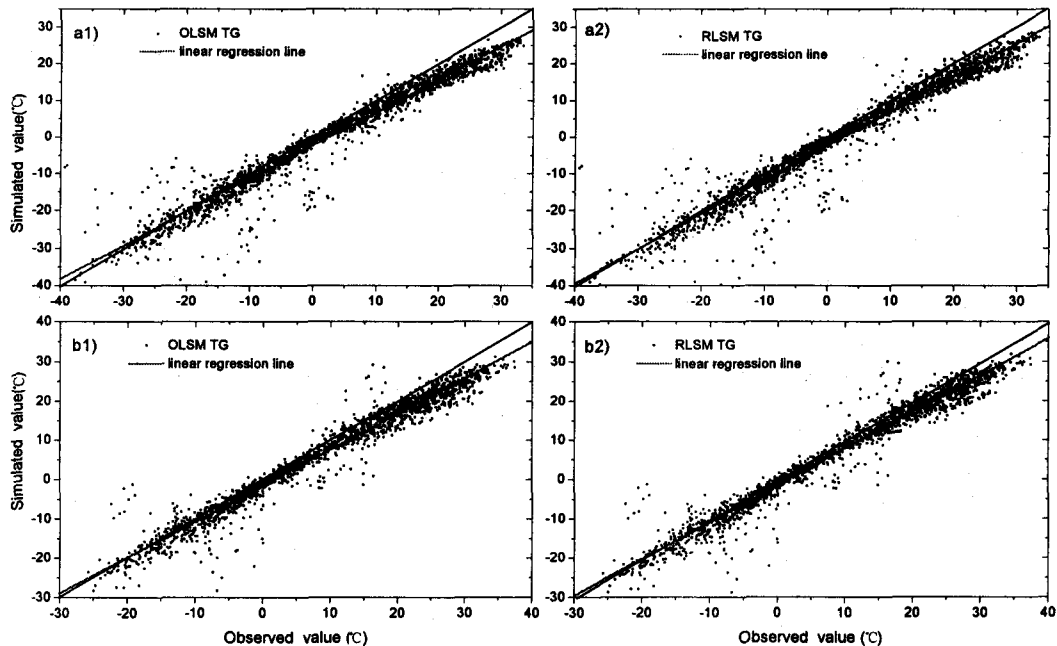


Fig. 10. Simulated (Y -axis) versus observed (X -axis) ground temperature for two stations. The 1:1 line and linear regression line are plotted on each panel. a1) and a2) are for Ogurtsovo; b1) and b2) are for Yershov.

is still frozen, and that causes increment in runoff, decrease in infiltration, and hardly simulates the replenishment of soil moisture in spring. Because it is lower in soil moisture and higher in ground temperature in the simulations by RLSM, the simulated latent heat is less and the sensible heat is higher.

There is some discussion about the soil moisture simulation in Robock et al. (1995) and Slater et al. (1998). It indicated that Bucket model without frozen soil process can simulate the ASM reasonably, and SSiB, in which all spring snowmelt is partitioned into runoff if the surface temperature is below the frozen point, cannot simulate the soil moisture spike in spring. Xue et al. (1996)^① modified the hydraulic conductivity using $K_{frz} = K_H [T_{soil} - (T_{frz} - 10)] / 10$, meaning that the hydraulic conductivity varies linearly in the range of -10°C – 0°C , and there were some evident improvements on the simulated results using the same forcing data as Robock et al. (1995). As described in Li and Cheng (1995), however, this consideration underestimates the effects of frozen soil, and it is hard to determine the basic range of the order of magnitude according to current data.

The authors would like to thank Professors Sun Shufen and Li Shuxun for their valuable suggestion. Professor Alan Robock generously provided the Former Soviet Union observational data. This study is supported by National Key Developing Programme for Basic Sciences (G1998040900) and the Innovation Project of Cold and Arid Regions Environment and Engineering Research Institute, CAS (CACX210036).

^①We have not found the original copy of this paper, but there is some discussion in Slater et al. (1998).

REFERENCES

- Bonan, G. B., 1996: A Land Surface Model (LSM version 1.0) for Ecological, Hydrological, and Atmospheric Studies: Technical Description and User's Guide, NCAR Tech Note NCAR/TN417+STR.
- Cherkauer, K. A., and D. P. Lettenmaier, 1999: Hydrologic effects of frozen soils in the upper Mississippi River basin. *J. Geophys. Res.*, **104**, 19599–19610.
- Clapp, R. B., and G. M. Hornberger, 1978: Empirical equations for some soil hydraulic properties. *Water Resour. Res.*, **14**, 601–604.
- Cosby, B. J., G. M. Hornberger, R. B. Clapp, and T. R. Ginn, 1984: A statistical exploration of the relationships of soil moisture characteristics to the physical properties of soils. *Water Resour. Res.*, **20**, 682–690.
- Dickinson, R. E., A. Henderson-Sellers, and P. J. Kennedy, 1993: Biosphere–Atmosphere Transfer Scheme (BATS) version 1e as coupled to the NCAR Community Climate Model, NCAR Tech. Note. TN-387+STR, 72pp.
- Farouki, O. T., 1981: The thermal properties of soil in cold regions. *Cold Regions Sci. Tech.*, **5**, 67–75.
- Farouki, O. T., 1986: *Thermal Properties of Soils*. Series on rock and soil mechanics, Vol.11. Trans. Tech. Pub., 136pp.
- Guymon, G. L., and J. N. Luthin, 1974: A coupled heat and moisture transport model for arctic soils. *Water Resour. Res.*, **10**, 995–1001.
- Harlan, R. L., 1973: Analysis of coupled heat–fluid transport in partially frozen soil. *Water Resour. Res.*, **9**, 1314–1323.
- Jame, Y. W., and D. I. Norum, 1980: Heat and mass transfer in a freezing unsaturated porous medium. *Water Resour. Res.*, **117**, 811–819.
- Johanson, O., 1975: Thermal conductivity of soils. Ph. D. dissertation, University of Trondheim, 236pp.
- Kennedy, I., and B. Sharatt, 1998: Model comparison to simulate soil frost depth. *Soil Science*, **163**, 636–645.
- Koren, V., and J. Schaake, K. Mitchell, O. Y. Duan, F. Chen, and J. M. Baker, 1999: A parameterization of snowpack and frozen ground intended for NCEP weather and climate models. *J. Geophys. Res.*, **104**, 19569–19585.
- Li Shuxun, and Cheng Guodong, 1995: *Problem of Heat and Moisture Transfer in Freezing and Thawing Soils*. Lanzhou University press, 203pp.
- O'Neill, K., and R. D. Miller, 1985: Exploration of a rigid–ice of frost heave. *Water Resour. Res.*, **21**, 281–196.
- Pauwels, V. R. N., and E. F. Wood, 1999: A soil–vegetation–atmosphere transfer scheme for the modeling of water and energy balance processes in high latitudes. 1. Model improvements. *J. Geophys. Res.*, **104**, 27811–27822.
- Peter–Lidard, C. D., E. Blackburn, X. Liang, and E. F. Wood, 1998: The effect of soil thermal conductivity parameterization on surface energy fluxes and temperatures. *J. Atmos. Sci.*, **55**, 1209–1224.
- Robock, A., K. Y. Vinnikov, C. A. Schlosser, N. A. Speranskaya, and Y. Xue, 1995: Use of midlatitude soil moisture and meteorological observations to validate soil moisture simulations with biosphere and bucket models. *J. Climate.*, **8**, 15–35.
- Schlosser, C. A., A. G. Slater, A. Robock, A. J. Pitman, K. Y. Vinnikov, A. Henderson–Sellers, N. A. Speranskaya, K. Mitchell, and the PILPS 2(d) Contributors, 2000: Simulation of a boreal grassland hydrology at vaidai, russia: PILPS Phase 2(d). *Mon. Wea. Rev.*, **128**, 301–321.
- Sellers, P. J., D. A. Randall, G. J. Collatz, J. A. Berry, C. B. Field, D. A. Dazlich, C. Zhang, G. D. Collelo, and L. Bounoua, 1996: A revised land–surface parameterization (SiB2) for atmospheric GCMs. 1. Model formulation. *J. Climate*, **9**, 676–705.
- Slater, A. G., A. J. Pitman, and C. E. Desborough, 1998: Simulation of freeze–thaw cycles in a general circulation model land surface scheme. *J. Geophys. Res.*, **103**, 11303–11312.
- Sun, S. F., J. M. Jin, and Y. Xue, 1999: A simple snow–atmosphere–soil transfer model. *J. Geophys. Res.*, **104**, 19587–19597.
- Xue, Y., and J. Shukla, 1991: The influence of land properties on Sahel climate. Part I: Desertification. *J. Climate*, **6**, 2232–2245.
- Xue, Y., F. J. Zeng, and C. A. Schlosser, 1996: SSiB and its sensitivity to soil properties: A case study using

HAPEX-Mobihy data. *Global Planetary Change*, 13, 183-194.

Yang, Z. L., R. E. Dickinson, A. Robock, and K. Y. Vinnikov, 1997: Validation of the snow submodel of the biosphere-atmosphere transfer scheme with russian snow cover and meteorological observational data. *J. Climate*, 10, 353-373.

一个用于气候模式的简单冻土过程 参数化方案的建立和检验

张 宇 吕世华

摘 要

在 NCAR/LSM 的基础上,发展了一个简单的冻土过程参数化方案,并使用苏联 6 个站的水文气象观测资料考察了耦合了新方案模式的气候效应。在新方案中,加入了对含冰量的求解和在相变过程中的能量变化;并使用 Johanson 的方案替代了模式中原有的土壤导热率的参数化方案,考虑了含冰量对土壤水热性质的影响。原模式和改进后模式的模拟结果的比较得到,冻土过程方案能够合理的模拟土壤列中的能量收支及水热性质随含冰量的变化。随着入渗的减少和径流的增加,春季的土壤湿度减小。因此,热通量的分配和土壤温度也产生了相应的变化。

关键词: 冻土过程, 陆面过程模式, 气候模式